AIAA Propulsion and Energy Forum
19-22 August 2019, Indianapolis, IN
AIAA Propulsion and Energy 2019 Forum

10.2514/6.2019-4505



# Current Capabilities and Challenges of NDARC and SUAVE for eVTOL Aircraft Design and Analysis

J. Michael Vegh *
*U.S. Army Combat Capabilities Development Command Aviation & Missile Center, Aviation Development Directorate-Ames Moffett Field, CA 94035, USA*

Emilio Botero † Matthew Clark ‡, Jordan Smart §, Juan J. Alonso¶
*Stanford University, Stanford, CA 94305, USA*

**This paper compares and contrasts the application of two conceptual methods for the design and analysis of eVTOL aircraft. The starting point is a widely publicized reference design, the Kitty Hawk Cora, modeled using publicly available information. Using the two tools (NDARC and SUAVE), estimates of weight and performance of the aircraft for the same reference mission are made, highlighting areas of uncertainty based on differences in the observed results, with distinctions between design assumptions and modeling differences emphasized. Trade studies of gross takeoff weight vs. rotor radius and wingspan were performed to focus on the different sensitivities the models possess. For the initial designs, there was some agreement in overall gross takeoff weight despite different estimates for aerodynamic performance and component weights. While agreement was shown in terms of how rotor radius trades, the wingspan sweep showed opposing trends between these two codes. This paper details the reasons behind these disagreements and discusses particular disciplines that require closer scrutiny and further development using higher fidelity methods.**



## Nomenclature

| | | |
|---|---|---|
| AR | = | Aspect Ratio |
| DEP | = | Distributed Electric Propulsion |
| eVTOL | = | Electric Vertical Takeoff and Landing |
| GTOW | = | Gross Takeoff Weight |
| I | = | Inboard |
| M | = | Midboard |
| MTOW | = | Maximum Takeoff Weight |
| O | = | Outboard |
| RVLT | = | Revolutionary Vertical Lift Technology |
| Sref | = | Reference Area |
| t/c | = | thickness to chord ratio |
| UAM | = | Urban Air Mobility |
| VTOL | = | Vertical Takeoff and Landing |
| $W_{sys}$ | = | System weight |

## I. Introduction

THERE has been increasing interest in short range, on-demand air transportation in recent years [1–3]. To meet stringent design requirements, especially in terms of noise, range, and vehicle size, a variety of unconventional


*Aerospace Engineer, CCDC Aviation and Missile Center, Aviation Development Directorate-Ames, AIAA Member
†Ph.D. Candidate, Department of Aeronautics & Astronautics, AIAA Student Member
‡Ph.D. Candidate, Department of Aeronautics & Astronautics, AIAA Student Member
§Ph.D. Candidate, Department of Aeronautics & Astronautics, AIAA Student Member
¶Professor, Department of Aeronautics and Astronautics, AIAA Associate Fellow

configurations are being designed and tested. These configurations often require the use of higher-fidelity analysis to accurately capture the performance benefits of specific design choices, absent significant testing. Many proposed designs employ distributed electric propulsion (DEP). Distributed electric propulsion relies on a relatively large number of small electric motors/propellers rather than a single large propeller or rotor to fly the aircraft.

Cora, the reference design for this paper makes use of a DEP system with two separate sets of rotors: a VTOL system consisting of 12 rotors that are stopped during forward flight and a pusher propeller mounted on the rear of the fuselage. The rotary-wing design community refers to this configuration as a compound, stoppable-rotor helicopter. The baseline aircraft can be seen in Figure 1.

**Fig. 1 Kitty Hawk Cora (https://cora.aero/)**

Some publicly advertised geometry and performance data for the Cora may be seen in Table 1 [4]. From the reference data as well as known drawings/schematics, aircraft geometric parameters such as chord length, propeller length, and rotor position are estimated. These dependent geometric estimates are shown in Tables 2 and 3.

**Table 1 Cora Design Summary**

| | |
|---|---|
| Cruising Altitude | 500–3000 ft |
| Wingspan | 11 meters |
| Range | ≈ 100 km |
| Speed | ≈ 180 km/h |
| Number of Seats | 2 |

**Table 2 Aerodynamic Surface Geometry**

| **Parameter** | **Wing** | **Horizontal Stabilizer** | **Vertical Stabilizer** |
|---|---|---|---|
| $S_{ref}$ ($ft^2$) | 114 | 19.10 | 12.69 |
| AR | 11.4 | 4.78 | 1.41 |
| Taper | 1.0 | 1.0 | 0.5 |
| t/c | 0.18 | 0.12 | 0.12 |

**Table 3 Propulsor Geometry**

| **Parameter** | **Rotor** | **Propeller** |
|---|---|---|
| Solidity | 0.2 | 0.1 |
| Tip Radius (ft) | 2.0 | 3.5 |
| Taper | 0.75 | 0.8 |

The unconventional nature of the propulsor arrangement combined with battery technology limitations and required secondary systems are expected to present significant weights/loads/power issues that modern conceptual design techniques need to address. Additionally, previous work has shown that eVTOL aircraft are highly sensitive to how they are flown [5]. Because of this sensitivity to the mission, regulatory requirements (such as flying a specified distance above houses) may be a severely limiting constraint that sizes components in the final design. To be more specific, current FAA regulations for general aviation aircraft require a flight altitude of 1,000 ft above the highest obstacle in congested areas and 500 ft above ground level in less crowded areas[6]. Urban Air Mobility (UAM) regulations are expected to be similar, with a minimum cruise altitude of at least 500 ft [7]. Quickly climbing to cruise altitude in an urban setting can require significant power capability and can be a limiting constraint on the design.

This paper is a comparative study of two conceptual design tools, NDARC and SUAVE. The Cora serves as a vehicle for scrutinizing major differences across disciplines, as they are modeled and predicted by separately developed analysis frameworks. A primary goal of this work is to obtain estimates of some design metrics such as GTOW to emulate a "clean-sheet" design approach. It is hoped that, by comparing these estimates, the aircraft design community might become more aware of the specific challenges and weaknesses in evaluating the different, diverse concepts that are being proposed. It also acts as a case study as to how misapplication of conceptual tools or neglecting to model specific phenomena may lead to erroneous conclusions. Technologies and concepts developed in this Urban Air Mobility (UAM) framework may be of interest in future Army aircraft concepts. Understanding the strengths and weaknesses in current aircraft design frameworks could prove useful in evaluating these concepts. For the analysis here, a simplified version of the Uber Elevate nominal mission is used, with the mission profile shown in Figure 2 [1]. The mission payload is 400 lb.

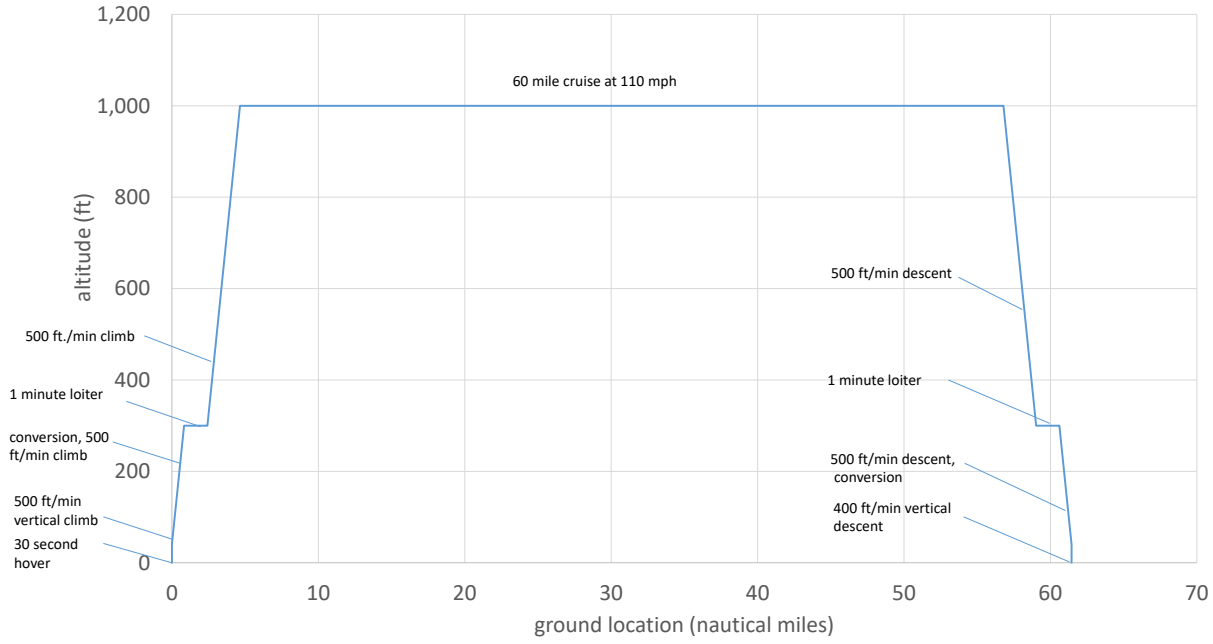


**Fig. 2 Simplified Uber Elevate Mission Profile Used for Comparative Design and Analysis of Cora Concept**

Results were compiled assuming a 300 W-h/kg (pack level) lithium-ion battery, with a 20% margin for cycle life. For the discharge models used in this report, this is roughly equivalent to a fully drained 240 W-h/kg battery. Battery specific power is assumed to be appropriately large in both toolchains to ensure robust convergence/design convergence and an ability to handle basic trade studies. Initial results indicated that battery specific power levels lower than $\approx 1.4$ kW/kg resulted in convergence issues in SUAVE for the baseline case; this suggests that specific power could be a limiting factor in some portions of the mission. Additionally, a constant 5hp load was used throughout the mission to model environmental conditioning.

Because of a lack of robust convergence in the hover and vertical climb segments in the SUAVE tool, rotor solidity was increased from 17% to 20% by decreasing the hub radius from 40% of the blade length to 32% of the blade length. This

may lead to insufficient motor cooling. However thermal effects are not currently modeled in either tool and are an important point of further study A graphic illustrating the changes to the rotor model can be seen in Figure 3.

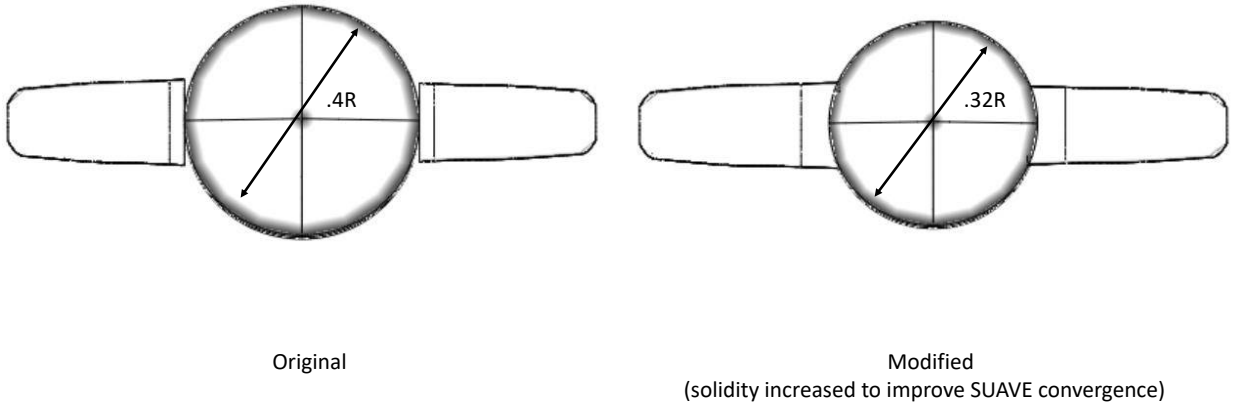


**Fig. 3 Baseline Rotor Change**

## II. NDARC Methodology

NDARC is a conceptual design environment capable of modeling a variety of aircraft, including tiltrotors, tailsitters, and helicopters [8]. Semi-parametric and parametric models are used to represent the aircraft. It employs a Newton-Raphson-based six-degree-of-freedom trim solver. Aircraft sizing is performed using successive substitution. Additionally, as a parametric system, weight, engine, as well as aerodynamics models may be readily tuned to match results from outside aerodynamics and comprehensive analysis such as CAMRAD II for rotor performance [9]. Follow-on work has extended NDARC's architecture to include models necessary to design electric and hybrid aircraft, along with efforts to model some candidate eVTOL configurations [10, 11]. Battery discharge losses are from an empirical lithium-ion discharge model, although the option to run the battery as an equivalent circuit exists. NDARC typically uses a calibrated parametric-based approach, where performance for a new design is estimated based on calibrating to other, similar aircraft at the component level. This is especially apparent in the weight modeling.

### A. Mission Performance

Aerodynamic calculations from NDARC use an assumed functional form (often a polynomial) based on multi-panel finite wing theory for the aerodynamic surfaces that can be tuned to data correlated from similar configurations to the aircraft of interest or collected from higher fidelity CFD data. Rotor performance uses parametric fits for profile, parasite and induced power that may be calibrated from comprehensive analysis such as CAMRAD II. Performance analysis for the configuration here was calibrated to the NASA Revolutionary Vertical Lift Technology (RVLT) models [12]. Typically, NDARC uses separate engine ratings for max rated and max continuous power to compute power available, both for conventional combustion-powered aircraft engines as well as for electric motors. However, because SUAVE does not distinguish between rating codes, it was decided to operate the motors at max continuous power throughout the mission, a conservative estimate.

### B. Weights

NDARC estimates vehicle weight at the component level defined by SAWE RP-8A using the AFDD 83-95 empirical weight models. These correlations are in turn based on fits of historical civil and military aircraft including turboshaft-

based helicopters as well as tiltrotors. The fuselage weight correlation was fit to a combination of 35 fixed wing aircraft and helicopters and has an average error of 6.5% over this dataset. The wing weight correlation (AFDD93) was fit to a combination of 25 fixed wing aircraft and possesses an error of 3.4 % over this dataset. Rotor weight is split into hub and blade components based on 51 aircraft with an average error of 7.9% for the blade and 12.2 % for the hub. To model the boom, the empennage was scaled such that it matches the combined boom and tail weight fraction of the North American Rockwell OV-10 with a tech factor improvement to account for the use of composites. Landing gear weight is parametric based on GTOW and wing loading, based on 28 aircraft and has an overall error of 8.4%. Wire weight is modelled as a fraction of installed battery weight; note that this is separate from the AFDD models and is a likely area of further development. To allow flexibility for the designer as well as model improvements in technology, tech factors are used to scale each component by a constant value to calibrate the baseline aircraft based on similar designs. They are also used to correlate to specific aircraft features, such as complexity.



## III. SUAVE Methodology

SUAVE uses a force-balance-based mission solver with a predefined number of collocation points for a given mission segment based on prescribed propulsion and aerodynamics modules which may be swapped out at will. To elaborate, an aircraft (such as a Cessna 172) may be simulated with a diesel engine in one instance, and, in a second instance use a fuel cell based propulsion system. In another case, a simple parametric module may be employed for one vehicle/mission combination while changing a single line of code runs the simulation using a high-fidelity CFD solver. An overview of analysis capabilities/methodologies of the environment can be found in Reference [13]. The capability to integrate higher-fidelity methods is documented in Reference [14]. Of note is that the current SUAVE toolchain may use OpenVSP to generate a geometric representation of the aircraft which can then meshed and used to call SU2 to run a higher fidelity CFD analysis [15, 16]. Sizing was performed using an optimizer-based decomposition approach [17], although in SUAVE, the option to reformulate and solve using Newton-Raphson's method and/or successive substitution exists [18].

Figure 4 visually describes SUAVE's energy network convergence procedure. On mission initialization the battery state and voltage are determined by user parameters, and thereafter derived from the aircraft force and propeller torque residuals. The battery is modelled using a Thevenin circuit which accounts for internal battery resistance and the resulting decrement to under-load network voltage. That is, as increasing power and torque are required, increased current is drawn from the battery, increasing losses due to internal resistance. The SUAVE mission solver accounts for this additional resistance and associated voltage drop when determining the actual voltage available to the propulsion system, and reports this result in addition to the open-circuit voltage across the battery terminals. In this way, voltage depletion constraints may be monitored and evaluated directly, though it implicitly imposes additional constraints on mission convergence. Battery performance estimation is further described in Reference [19].

### A. Mission Performance

For the work shown here, the Weissinger Vortex Lattice model is used for the wing. Drag losses for the rotors and landing gear are based on the excrescence area of these surfaces and bookkept as a drag increment. To estimate rotor and propeller performance, SUAVE utilizes a Blade Element Momentum-theory model with empirical corrections for hover [20]. Hover-cruise conversion performance is handled by a time-marching force balance.

### B. Weights

In contrast to NDARC, SUAVE utilizes a structural weight estimation based on physical material properties and estimated structural load, in addition to statistical weight regressions. This structural weight estimation methodology is an adaptation of a technique published by Airbus-A$^3$'s Project Vahana[21], modified to accommodate SUAVE's mission, analysis, and optimization structure. The methods have been designed to be operable either by accepting certain vehicle elements as fixed inputs, or else iteratively sizing certain elements until mission feasibility is achieved. They are principally based on limit-load sizing of various beam, keel, and skin thickness, taking into account yield and ultimate strength properties available in SUAVE's materials library. The limit load here was chosen to be 1.67 with a safety factor of 1.5 to match NDARC's choice for ultimate load of 2.5.

From an initial estimate of vehicle MTOW, SUAVE derives vehicle flight loads - a multiplicative factor applied to the MTOW estimate establishes the limit load for the vehicle which, in turn, allows for characterization of the spanwise lift distribution according to an elliptical profile. Modeled $C_L/C_D$ and $C_L/C_m$ ratios allow for estimates of drag and

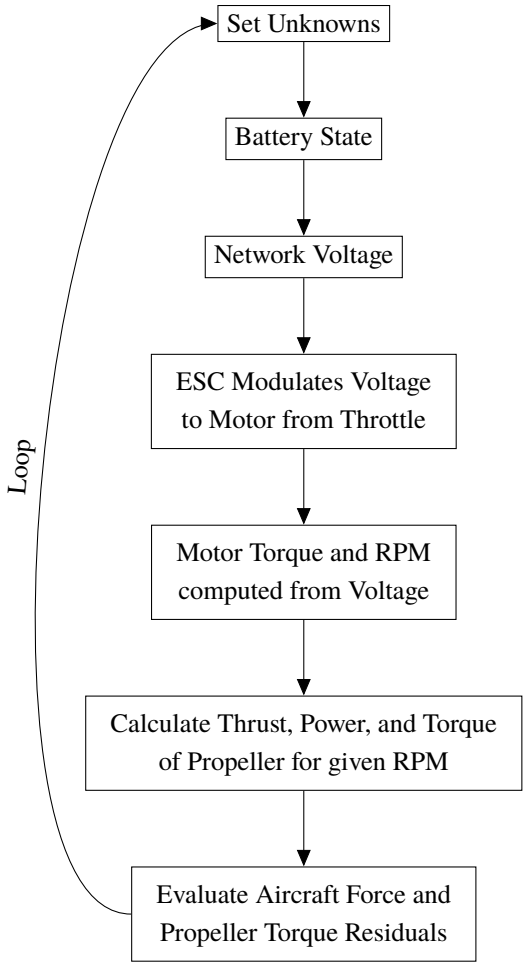


**Fig. 4 SUAVE Network Convergence Procedure**

moment distributions, and thus three-dimensional estimates of the shear, bending, and torsional loads on the wing are arrived at. Rotor loads are modeled by adding a shear to the spanwise rotor locations based on rotor thrust. Boom weight is indirectly modeled from these loads.

The comparative maximum at designated analysis points along the span of the wing is used to size the thickness of the outer skin, bending shear-carrying spars, and torsion box webbing. For this analysis, bidirectional carbon fiber composite is selected as the material for the primary load carrier throughout the wing, though skin weight also includes an allowance for an areal stack of carbon fiber reinforced polymer honeycomb core material, and an outer protective layer of vinyl, as well as epoxy necessary to join the materials. Ribs are modeled as I-beams using 6061-T6 aluminum with a minimum flange width of 25.4 mm.

The weight of individual blades of a rotor propeller are similarly sized, using the maximum thrust of the propeller to make an initial estimate of the propeller blade mass. Centripetal force is then calculated based on that estimate, and rotor components are sized based on a complete model of the shear, torsion, and axial forces experienced by the propeller in motion. If the mass buildup based on this sizing procedure agrees with the previous estimate to a relative tolerace of $10^{-8}$, the mass estimate is accepted. Otherwise, a new estimate of centripetal force is made using the buildup and the process procedes iteratively until convergence is achieved.

Of particular note is the addition of a 0.42 mm thick laminate of nickel-cobalt chromolybdenum alloy applied to the leading edge of each blade to protect it from damage against debris, rain, etc. While this element is frequently ignored in propeller weight estimation, the significant reduction in other structural weight afforded by the use of composite materials makes the addition of such leading edge protection a significant portion of overall rotor weight. 6061-T6 aluminum is used to model the root of the blade, sized to account for the axial centripetal force applied by the motion of

the propeller. Hub weight is set to a fixed input. To account for rotor pitch and roll moments during edgewise flight, a 15% factor is added to the baseline Vahana weight models for the rotors and associated hubs.

Fuselage weight is estimated from a combination of several sub-components, derived from an over-arching assumption that the fuselage is elliptical in form, characterized by a given length, width, and height. The root bending moment of the wing is used to estimate the necessary area and wall thickness afforded to a structural keel composed of unidirectional carbon fiber. The skin and bulkheads of the vehicle are, as with the wing, modelled as an areal stack of bidirectional carbon fiber composite, honeycomb carbon fiber reinforced polymer core material, a protective vinyl layer, and the epoxy necessary to join the materials. The canopy is modelled as occupying 1/8th the wetted area of the fuselage, and composed of polymethyl methacrylate. Additionally, landing impact loads are used to size steel bolts and bidirectional carbon fiber laminate pads capable of supporting the vehicle. Landing gear weight is simply estimated as a fixed 2% of overall GTOW (which is optimistic).

Communication wiring and power cabling is sized based on the geometry of the fuselage and relative position of each motor. Based on the maximum expected power draw from the motors, and the limiting power density of copper wiring, necessary cable thickness is multiplied by length to reach the motors from the battery, providing an estimate of cable weight. Communication wire is similarly based on an assumed density of fiber-optic wiring necessary to carry signals around a network sized based on fuselage geometry.

The non-geometric buildup includes such items as seats, avionics, motor and servo weights, a ballistic recovery system, landing gear, etc. Seats and servomotors are a fixed per-passenger/per-motor additional weight. A notable absence is the lack of an explicit allowance for environmental control systems or other onboard systems which the authors view as a critical component to allow for acceptable levels of passenger comfort and mitigation of motion sickness. Thus SUAVE adopts the same correlative systems weight estimate as NDARC for this study. The linear fit based on NDARC's systems weight assumptions for this aircraft, is shown in Equation 1.

$$W_{sys} = 0.0239 * GTOW + 195.71 \tag{1}$$

where GTOW and $W_{sys}$ are both in lb. Empennage weight is based on a general aviation correlation from Reference [22]. A more detailed explanation of SUAVE's eVTOL weight estimation method including formulas and implementation is available in Reference [23]. One significant change from the Vahana model is that normally, the Vahana models use a 10% contingency based on empty weight for the sake of conservatism; here, that contingency is removed to attempt to make a more accurate comparison. One other area where SUAVE is made to match NDARC more closely is in the motor model. Motor weight is dependent on torque, and from the NDARC theory manual is computed as

$$W_{motor} = 0.3928Q^{.8587} \tag{2}$$

where Q is in ft-lb and $W_{motor}$ is in lb. This relation for high-torque-to-weight motors is based on 25 motors and possesses an average error of 21.8% over this dataset. SUAVE's python-based, extensible framework makes changes to the source code such as these a trivial exercise.

## IV. Methodology Comparison Summary

An overview of the design approaches used in NDARC and SUAVE can be seen in Sections II and III. This section includes a discussion of some of the key difference between the codes. Table 4 highlights the differences in weight methodology based on the component. Now, it should be noted that for SUAVE as well as NDARC, other choices for the component weight modeling may be used. The choices in Table 4 are simply, in the view of the authors, the best choice to model this particular eVTOL aircraft.

One of the primary challenges when it comes to comparing two different design tools is to ensure consistent bookkeeping, especially for these new configurations for which no current standard exists. The Society of Allied Weight Engineers offers some guidance, but not for an electrically propelled and controlled aircraft. Additionally, it should be noted that Mil-STD 1374B has a convention for weights that allows for consistent comparison with aircraft, but in many cases, when building statistical regressions, engineers may use their own bookkeeping choices that do not fall under said standard.

Nonetheless, efforts were made to ensure that technology/performance assumptions are matched between the two designs. Structural weight is one example where there is a larger degree of uncertainty due to the vastly different approaches that the two design codes employ. In NDARC, tech factors are used to model a largely composite aircraft with a 24% reduction in fuselage weight and 35% reduction in weight compared to an aluminum structure. The SUAVE

**Table 4 Weight Methodology Summary**

| Component | NDARC | SUAVE |
|---|---|---|
| Structural Weight (Wing) | Parametric (from 25 fixed wing aircraft) | Buildup from 3D shear, bending, torsional loads (Vahana) |
| Structural Weight (Fuselage) | Parametric (mix of 35 fixed wing and helicopter) | Buildup from 3D shear, bending, torsional loads (Vahana) |
| Structural Weight (Empennage) | Parametric (calibrated to OV-10 with material improvement) | General aviation correlation (Raymer) |
| Rotor Weight | Parametric from 51 aircraft | Converged based on centripetal force (Vahana) |
| Hub Weight | Parametric from 35 aircraft | Fixed input |
| Contingency Weight | None | None |
| Wiring Weight | Included in installation weight | From fuselage geometry and motor locations |
| Environmental Conditioning | Fixed input | None by default, fixed input here |
| Aircraft Sizing | Fixed point iteration | Optimizer decomposition |



models here employ a carbon fiber structure with aluminum ribs. Ensuring a confident, consistent comparison requires much more detailed analysis beyond the scope of this paper. Wiring weight is another area of uncertainty as, due to the sparsity of electric aircraft, there are a lack of reliable empirical relations to draw from. Furthermore, as of the time of writing, there is no consensus as to what constitutes an airworthy electric system. Sizing is typically performed using fixed point iteration in NDARC and optimizer decomposition in SUAVE, although the option to wrap NDARC in external codes such as rcotools and OpenMDAO and converge the problem using an optimizer exists [24, 25]. SUAVE includes an option for a native fixed point iteration solver, but this option is not employed here. A comparison of mission performance methodology can be seen in Table 5.

**Table 5 Performance Methodology Summary**

| Discipline | NDARC | SUAVE |
|---|---|---|
| Rotor Model | Profile, parasite, and induced power surrogates calibrated to CAMRAD II results | Blade element model with empirical hover correction |
| Hover-Cruise Conversion Dynamics | Quasi-Steady Trimmed | Collocation point based dynamic simulation |
| Wing Aerodynamics | Finite wing theory with calibratible parametric models and multiple panels | Weissinger Vortex Lattice with multiple panels |
| Battery Discharge Modeling | Empirical resistive losses with C-rate and state of charge | Mission solver determines current and voltage with empirical resistive loss model |

Several important modeling differences exist between these two tools. One example is how the conversion from hover/rotor-borne flight to wingborne flight occurs. This is typically modeled in SUAVE via a constant pitch-rate constant acceleration segment of .2g. In NDARC conversion was not modeled directly, but instead, to ensure this capability in the aircraft, margin was built into the rotor and electric motor system. Some trends from Tables 4 and 5 are that, in general, SUAVE's methodology tends to be less empirically-based than NDARC's: underlying disciplines tend

to rely more directly on "physics" in SUAVE, although most of NDARC's correlations are semi-empirical, so they have some physical basis as well. For any design tool the user must be careful when applying a given model, even a higher fidelity model for a number of reasons. Namely, incorporating higher fidelity methods leads to more points of failure from a numerical standpoint, leading to less robust behavior. Furthermore even good physics-based models can lead to spurious results when misused. For example, previous versions of SUAVE used a simple blade element momentum theory model in hover (a fundamental misapplication), yielding an unrealistic Figure of Merit of .88. The analogy-based approach employed in the NDARC models here means that, properly calibrated, this tool is likely more accurate than SUAVE in a given situation. However, this need for calibration often requires greater expertise on the part of the user to obtain meaningful results. As discussed in Section II, the rotor models in NDARC were calibrated to a comprehensive analysis (CAMRAD II), so hover performance estimation of these aircraft from NDARC is more credible. However, the lack of data on similar aircraft configurations means a lower level of confidence in the weight estimates; as a result, discrepancies between the semi-empirical parametrics of NDARC and the more physics-based SUAVE models are an important area to investigate. While SUAVE possesses the capability to compute the full conversion from the hover configuration (where the rotors are operated) to the cruise configuration (where the rotors are stopped and the wing carries the lift), to ensure a more accurate comparison of the underlying methodology, this option was not utilized here.



## V. Comparison of Results

The baseline system weights (from NDARC) can be seen in Table 6. Recall that these combined weights are used to create the linear fits for the SUAVE systems weight in Equation 1 and are identical for both software tools in this study. A summary of some of the most important aircraft performance estimates for each code can be seen in Table 7.

**Table 6 Baseline NDARC System Weights (lb)**

| | |
|---|---|
| flight controls | 133 |
| instruments | 10 |
| electrical group | 6 |
| avionics (MEQ) | 40 |
| furnishings and equipment | 30 |
| environmental control | 30 |
| total systems | 249 |

**Table 7 Baseline Performance Summary**

| **parameter** | **NDARC** | **SUAVE** |
|---|---|---|
| GTOW (lb) | 2,233 | 2,086 |
| Structural Weight (lb) | 715 | 505 |
| L/D (Cruise) | 11.5 | 9.70 |
| Propulsive Efficiency (Cruise) | 0.839 | 0.807 |
| $\eta_{motor} * \eta_{battery}$ (Cruise) | 0.888 | 0.904 |
| Hover Figure of Merit | 0.673 | 0.601 |
| Aircraft Power Loading (lb/hp) | 5.94 | 5.52 |

In general, aircraft performance estimates from NDARC are more optimistic than from SUAVE, particularly when it comes to aerodynamics, where the predicted lift-to-drag ratio in cruise from NDARC is nearly 20% higher than in SUAVE. However, the predicted gross takeoff weights are nearly identical. This could exemplify one common phenomena in conceptual design in that, although certain component/discipline uncertainties may be relatively large, they often cancel each other out. This phenomena can be readily seen in Table 7, where the cruise performance in NDARC is much more optimistic than SUAVE, yet the gross takeoff weights are very similar. To help understand the

aerodynamic performance disparity, a drag breakdown comparison (in flat plate area) between the two tools at the cruise condition can be seen in Figure 5.

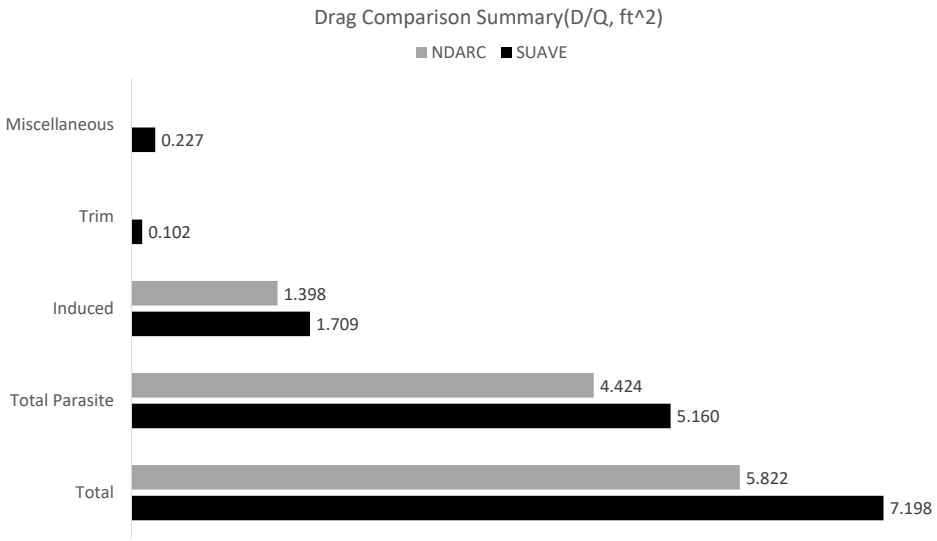


**Fig. 5 Drag Breakdown Summary**

Note that compressibility effects are neglible at the flight regimes here, so they are neglected in the reporting. Aerodynamic performance estimation from NDARC reflects conscious optimism on the part of the designer, whereas aerodynamic estimation from SUAVE comes from a more standardized aerodynamic computation. The aerodynamics bookkeeping methodologies are somewhat different between the two tools. One significant example of this is the drag from the rotors in edgewise flight; in SUAVE, this is computed using a drag increment based on excrescence area (along with the landing gear), while in NDARC, this is computed using a constant skin friction coefficient and lies within the parasite drag D/Q. Parasite drag D/Q is broken down by component in Figure 6, where I, M, and O refer to the inboard, midboard, and outboard location.

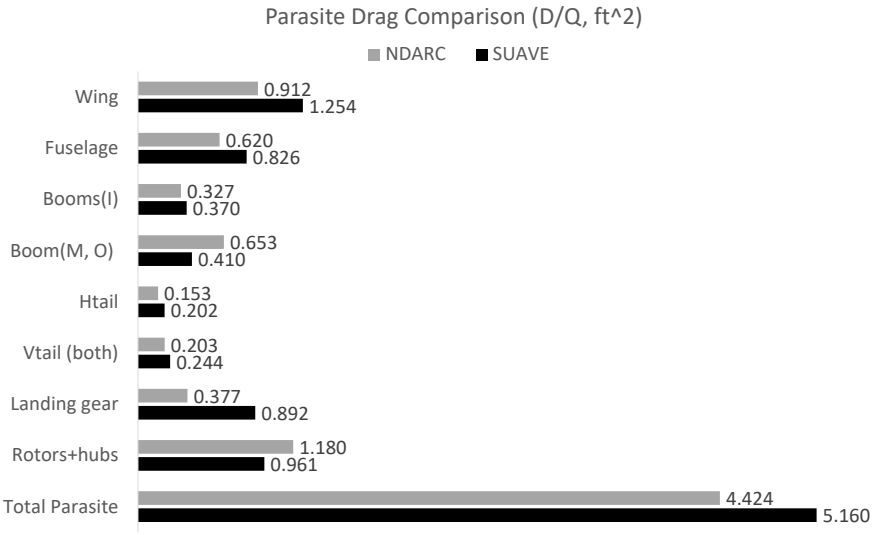


**Fig. 6 Parasite Drag Breakdown**

A quick comparison of Figures 5 and 6 shows that parasite as well as induced drag estimates from SUAVE are significantly larger. Furthermore, even for relatively well-understood features, such as the wing, there is substantial disagreement. In addition, the induced drag predicted by SUAVE is about 20% higher than that of NDARC. Notably, the landing gear drag predicted by SUAVE is over twice that predicted by NDARC, which contrasts with the other components where NDARC predicts consistently lower drag. In total, this 22% drag difference in cruise between the two software packages is an important area of scrutiny. In part, it is a result of the aggressive aerodynamic assumptions of these eVTOL NDARC models. Despite this disagreement, the overall predicted GTOW is similar. To understand this, one must look at the weight breakdown. Table 8 shows an overall summary of the aircraft weights.

**Table 8 Weight Comparison**

| parameter | NDARC | SUAVE | difference |
|---|---|---|---|
| GTOW | 2,233 lb | 2,086 lb | 0.068 |
| Empty Weight | 1,834 lb | 1,686 lb | 0.084 |
| Structural Weight | 701 lb | 505 lb | 0.324 |
| Propulsion System Weight | 866 lb | 928 lb | 0.069 |
| Payload Weight | 400 lb | 400 lb | N/A |

While gross takeoff weight estimates between the two methodologies are similar, the structural weight fraction in SUAVE is significantly smaller. Here, structural weight is defined as the weight of the wing, fuselage, empennage, rotors, and landing gear. A component-based breakdown can be seen in Table 9.

**Table 9 Empty Weight Component Breakdown**

| component | NDARC | SUAVE | difference |
|---|---|---|---|
| Wing+Booms+Empennage | 276 lb | 239 lb | 0.141 |
| Fuselage | 167 lb | 127 lb | 0.271 |
| Motor System | 494 lb | 485 lb | 0.019 |
| Battery Weight | 372 lb | 444 lb | 0.174 |
| Rotors/Propeller | 116 lb | 101 lb | 0.136 |
| Systems/Equipment | 249 lb | 245 lb | 0.016 |
| Landing Gear | 141 lb | 37 lb | 1.165 |
| Empty Weight (Total) | 1,831 lb | 1,686 lb | 0.084 |

One can see from Tables 8 and 9 that the percentage difference in GTOW between the two methodologies is around 7% and substantial differences exist across all major components (other than the motor, where both tools use the same weight correlation), which indicates a high degree of uncertainty. Furthermore, the percentage difference across all structural components is well outside the average error of all of the NDARC empirical correlations (3.4% for the wing, 6.5% for the fuselage, 7.8% for the rotor blade, 12.2% for the hub, and 8.4% for the landing gear). The largest difference comes from the landing gear, which in SUAVE (from the Vahana correlations) is a fixed 2% of GTOW, but here, is 100 lb lighter than NDARC's, suggesting that the 2% assumption is overoptimistic. The battery weight difference is in large part a result of the differing cruise performance, and reflects a total installed capacity of 183 MJ from NDARC and 218 MJ from SUAVE (147MJ and 174MJ are used to fly the mission, respectively). Total structural weight from NDARC is 200 lb heavier than SUAVE, with about half of that coming from the difference in landing gear weight. This suggests a substantial degree of optimism in the SUAVE models that the NDARC models do not possess; it bears noting that the SUAVE weight models here assume a largely carbon fiber structure. A visual representation of the weight breakdown can be seen in Figure 7.

Now, in contrast to many electric aircraft design studies[26–29], the motor, rather than the battery, is the heaviest component on the aircraft, based on estimates from both toolsets. This is because the aircraft uses direct drive motors,

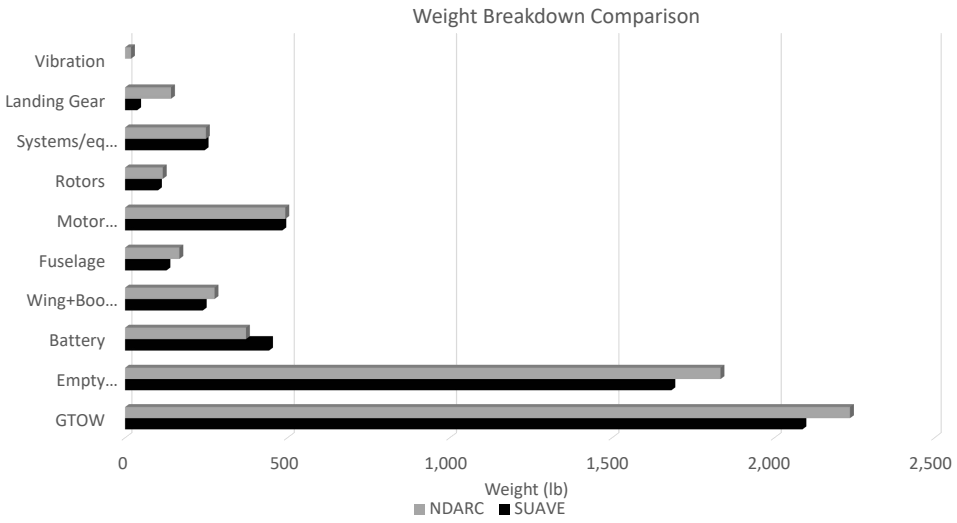


**Fig. 7 Weight Breakdown**

which, from existing trends, will be heavier than a motor-transmission system [12]. This means that properly estimating torque requirements in hover and takeoff becomes critical. Notably, these estimates are often neglected in other eVTOL design studies. The battery and motor combined constitute around 40% of the gross takeoff weight of both designs.

One important characteristic of these eVTOL designs is that, because of specific energy limitations, overall aircraft range is much lower than passenger aircraft. As a result, a relatively smaller portion of the mission is spent in the more aerodynamically efficient cruise segment. Depending on the target range of these aircraft, improving performance at the takeoff, climb, and descent conditions become comparatively more important. To illustrate, a bar chart comparing overall energy usage in each segment can be seen in Figure 8.

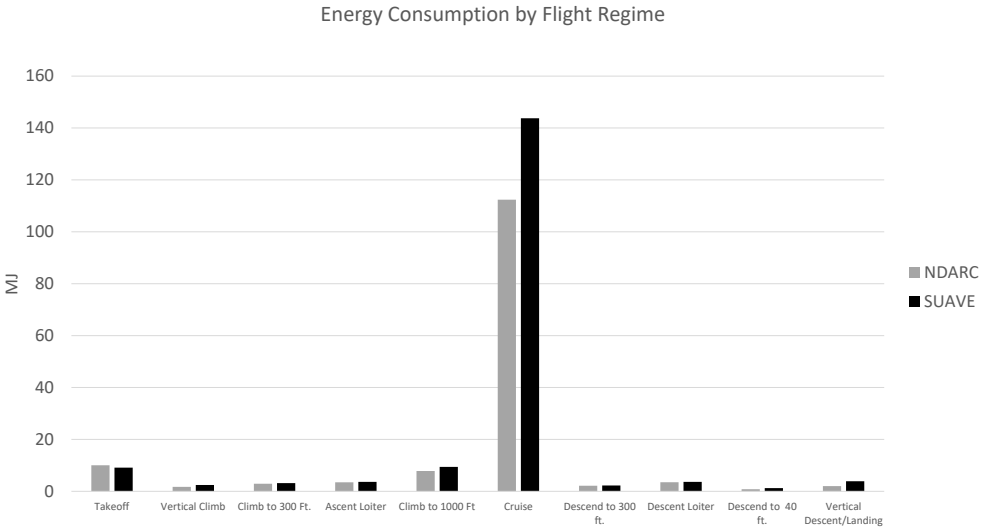


**Fig. 8 Energy Usage**

From Figure 8, both tools predict that around 75-80% of the energy usage would be at the cruise condition. The less optimistic aerodynamic assumptions from SUAVE are apparent here, where the energy usage in cruise is about 20%

higher in SUAVE because of the drag differences (See Figures 5 and 6). It should also be noted that accurately modeling hover and climb performance are important not only for the energy usage, but also because they tend to size significant sections of the aircraft such as wiring (here, a part of installation weight), electric motors, and in some instances, the battery. Table 9 illustrates how power requirements between the two codes differ by flight regime.

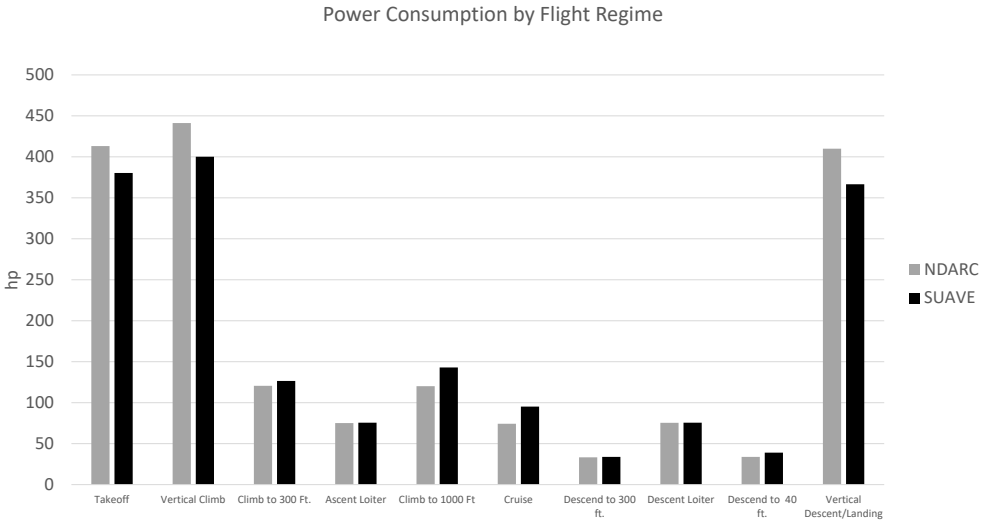


**Fig. 9 Power Required**

One will notice that the predicted power requirements in hover for NDARC are greater than SUAVE despite the higher Figure of Merit (see Table 7); this is because the SUAVE aircraft possesses a higher battery/electronic system efficiency during these flight conditions (82% in hover in NDARC vs. 90% in SUAVE). In addition, the NDARC aircraft is 7% heavier. SUAVE uses lower aerodynamic performance assumptions, which is apparent from the fact that it predicts a higher power consumption during wing-born flight. As is evident from these results, electric system performance estimation (especially the battery and motor) are an important aspect of electric aircraft design. Figure 10 depicts the battery performance characteristics as the mission progresses.

Qualitatively speaking, the performance estimation of the battery system between the two toolchains is similar (except at the vertical climb and descent conditions), which strongly contrasts with the drag breakdown or the weight statement. In this study, the NDARC uses an empirical resistive loss model, with power flowing to a motor model with a fixed 95% efficiency, while SUAVE estimates the voltage drop across the battery, the speed controller, and the avionics, which ramps up and down throughout the mission. Now, one should note that operating an aircraft with the C-rates predicted by NDARC result in a low battery life. Recall that C-rate refers to the time to discharge a battery at a given condition in 1/hour; a C-rate of 1 means that the battery discharges in one hour, while a C-rate of 2 means that the battery discharges in 30 minutes. SUAVE possesses a larger battery and predicts a more efficient electrical system during high power operation. As a result, in NDARC, the C-rates are much lower in the hover, vertical climb, and vertical descent segments. The generous battery assumptions employed here lead to the baseline aircraft from NDARC sizing to a case where cycle life would be too low for long-term operational use.

### A. Trade Studies

A plot showing the sensitivity of GTOW to rotor radius can be seen in Figure 11. Solidity was maintained for all of the designs.

Here, both toolsets predict a lighter aircraft with shrinking rotor radius (although NDARC predicts a local optimum). Interestingly, although currently, drag from the rotor is bookkept in increment drag which does not scale with rotor radius, SUAVE's weight prediction seems to be more sensitive to this trade. The primary impact of changing the rotor radius on these models comes from increasing rotor and motor weight; larger rotors require more torque from the motors, meaning a heavier propulsion system. One important area of difference between the two codes is the rotor tip

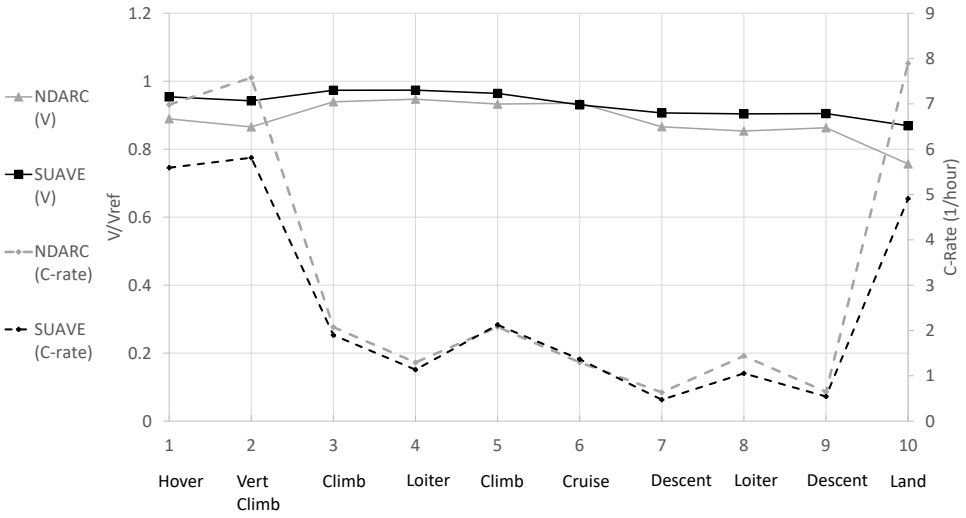


**Fig. 10 Battery Characteristics**

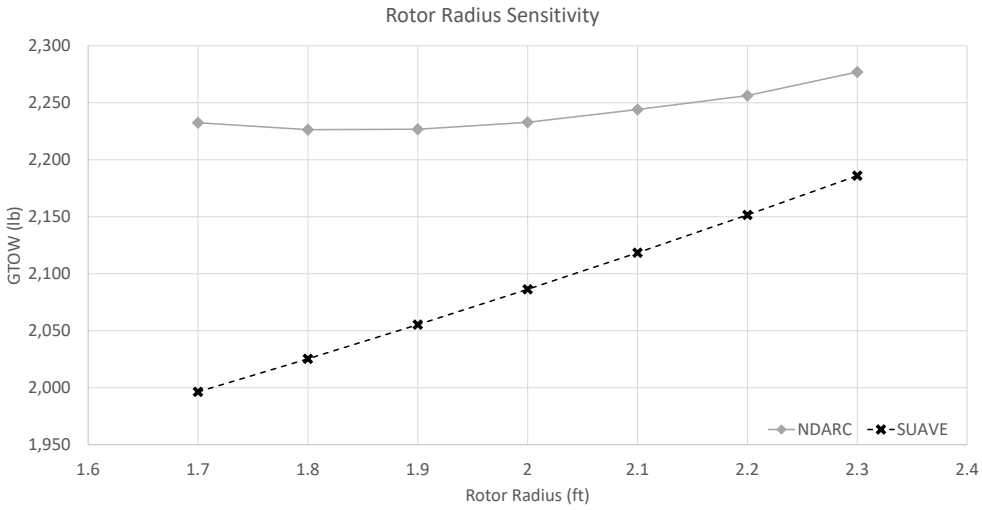


**Fig. 11 Rotor Radius Sweep**

speed; SUAVE estimates a tip speed of 470 ft/s in hover, while NDARC predicts a tip speed of 650 ft/s. The lower tip speed prediction in SUAVE is likely due to a lower blade pitch value in the rotor model, as NDARC is using a collective of 13.5 degrees. Additionally, this tip speed results in a higher predicted torque in SUAVE despite the roughly equal motor weights and identical motor weight model. This discrepancy should be followed up on in an actual aircraft design program.

A plot of GTOW vs wingspan can be seen in Figure 12. Wing area was kept constant, while aspect ratio was changed. Here, one should immediately notice that NDARC and SUAVE predict the opposite performance trends with wingspan. This is because in SUAVE, wing weight (baseline 240 lb, including the boom loads) is a substantial fraction of the structural weight of the vehicle, while induced drag is a comparably small fraction of total drag. In NDARC, on the other hand, wing weight without the boom and empennage modeled accounts for only 115 lb for the baseline case; therefore, for the way this aircraft is modeled in NDARC, the reduction in parasite drag is more significant than the

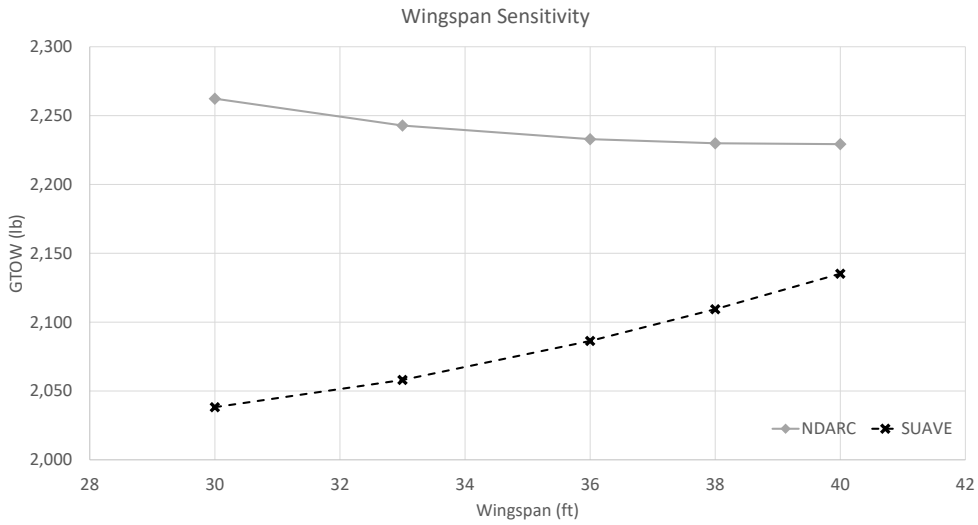


**Fig. 12 Wingspan Sweep**

structural weight tradeoff. This can be seen more clearly in Figure 13 which shows how the wing and empennage weight fraction trades with wingspan.

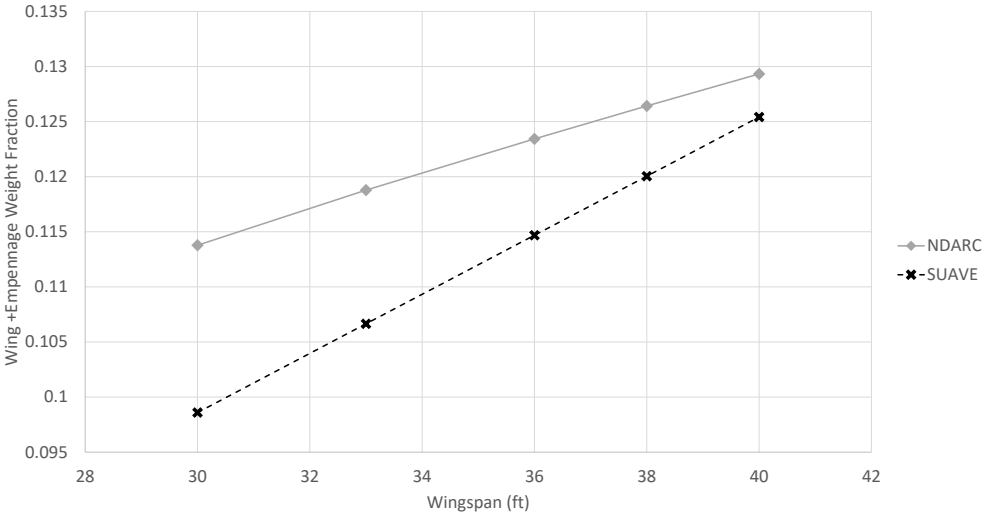


**Fig. 13 Wingspan vs. Wing+Empennage Weight Fraction**

While both tools predict an increasing structural weight fraction with wingspan (as would be expected), the slope of the results from SUAVE is steeper. This is because SUAVE is directly computing the rotor loads along the span of the wing while the NDARC model is calibrated based on the combined wing and empennage weight; the weight model for the empennage does not change with wingspan. As result, some of the physical effects are not captured here, so the SUAVE wing weight trend is likely more reliable. However, as rotor interactional effects are not modeled in SUAVE, there are still important physics missing that may affect the results of this trade.

## B. Optimization

As a further point of comparison between SUAVE and NDARC, a simple optimization problem was created starting from the baseline aircraft where rotor radius and wingspan were the design variables and wing area was kept constant. Rotor radius was bounded between 1.7 and 2.5 feet while wingspan was bounded between 30 and 40 feet. A constraint was added on wingspan and rotor radius to ensure rotor clearance. The gradient-based optimizer SLSQP was used to perform the optimization [30]. Results for this optimization problem can be seen in Table 10.

**Table 10 Aircraft Summary**

| Aircraft | Rotor Radius | Wingspan | DGW |
|---|---|---|---|
| Baseline (NDARC) | 2.00 ft | 36.0 ft | 2,233 lb |
| Baseline (SUAVE) | 2.00 ft | 36.0 ft | 2,086 lb |
| NDARC Optimum | 1.83 ft | 39.5 ft | 2,223 lb |
| SUAVE Optimum | 1.70 ft | 30.0 ft | 1,948 lb |
| NDARC at SUAVE Optimum | 1.70 ft | 30.0 ft | 2,267 lb |
| SUAVE at NDARC Optimum | 1.83 ft | 39.5 ft | 2,075 lb |

Table 10 illustrates some likely shortcomings of modeling choices in both toolchains. SUAVE's optimum lives at the lower boundary of rotor radius and wingspan, while NDARC's optimum is at a radius of 1.83 ft and wingspan of 39.5 ft. Here, because the NDARC model appears to be insensitive to major design choices such as rotor radius and wingspan; an optimization of the design only yields a change in DGW of 10 lb, which is exceedingly small considering the range factors that one tends to encounter in electric aircraft (unless the baseline aircraft was already nearly a local optimum, which is a possibility). Regardless, the opposing trend in wingspan is the most significant tradeoff here. While sizing the NDARC-optimal aircraft in SUAVE results in a gross takeoff weight nearly identical to SUAVE's baseline estimate, running NDARC based on SUAVE's optimum rotor radius and wingspan results in an aircraft that is 30 lb heavier. This is significant considering the relatively modest gains NDARC predicts from an "optimal" aircraft. Figure 14 depicts the geometry of the baseline aircraft, the NDARC-optimal aircraft, and the SUAVE-optimal aircraft.

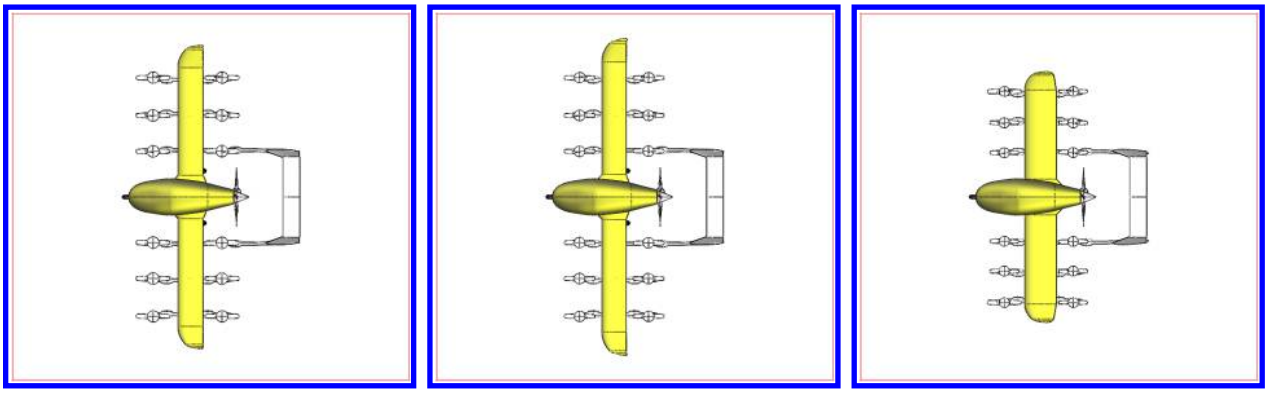

**(a) Baseline Aircraft** **(b) NDARC Optimum** **(c) SUAVE Optimum**

**Fig. 14 Wingspan and Rotor Radius Optimization**

Note that, to generate Figure 14c, the rotors needed to be moved closer together. The interactional effects were not modeled here; as a result, the weight benefits from the reduced spanwise wingloading are likely less significant than the results from Table 10 would suggest. Additionally, the substantial differences between Figures 14b and 14c demonstrate some of the difficulties of modeling complicated configurations without previous designs to calibrate to. Nonetheless, the fact that both tools predict that motor weight tends to drive the design suggest that this is a potential area of improvement for this aircraft; as these motors are sized by torque, the introduction of a gearbox may potentially result in a lighter aircraft from a systems-level perspective.

Additionally, because of the specific power battery assumptions, the C-rate in the NDARC designs are too high for

operational use. In essence, this unphysical assumption drives the design to a smaller rotor; without the battery limits or other constraints, the tradeoffs associated with this higher disk loading are not modeled. To illustrate the effect a more reasonable battery assumption has on the design tradeoffs, constrained optimization problems where C-rate is set to <6 are solved. Table 11 summarizes the results when the designs are limited to a maximum C-rate of less than 6. Here, the baseline aircraft in NDARC requires an additional 200 lb of weight to account for the larger battery. SUAVE's baseline weight estimate meets this constraint. A side-by-side comparison of these aircraft can be seen in Figure 15.

**Table 11 C-rate Constrained Aircraft Summary**

| Aircraft | Rotor Radius | Wingspan | DGW |
|---|---|---|---|
| Baseline (NDARC) | 2.00 ft | 36.0 ft | 2,397 lb |
| Baseline (SUAVE) | 2.00 ft | 36.0 ft | 2,086 lb |
| NDARC Optimum | 2.47 ft | 38.7 ft | 2,308 lb |
| SUAVE Optimum | 1.70 ft | 30.0 ft | 1,948 lb |
| SUAVE at NDARC Optimum | 2.47 ft | 38.7 ft | 2,281 lb |

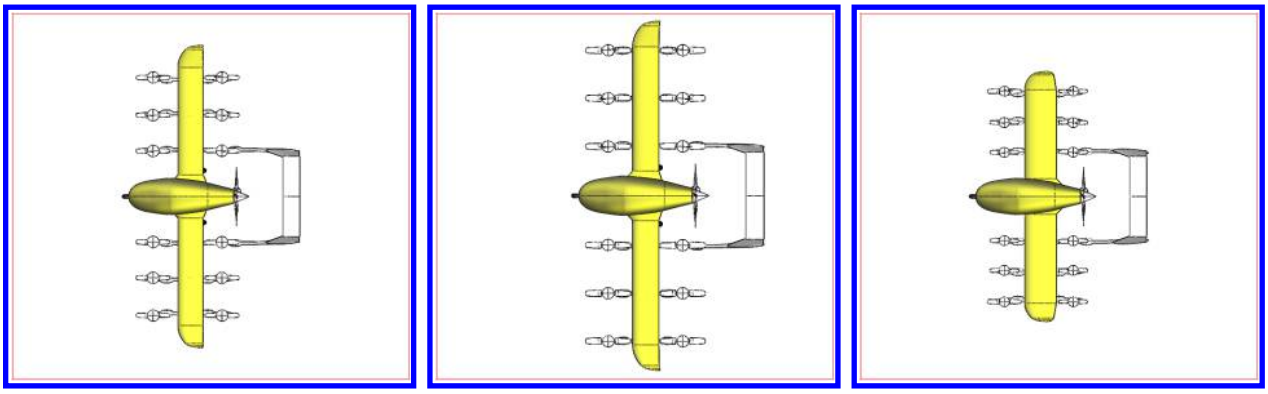

**(a) Baseline Aircraft** **(b) NDARC Optimum** **(c) SUAVE Optimum**

**Fig. 15 C-rate Constrained Optimization**

Including the C-rate constraint in the design fundamentally changes how the NDARC design trades; this constraint drives the aircraft to a lower disk loading with a corresponding span increase to allow for rotor tip clearance. SUAVE's optimum design from Table 10 meets this constraint, so the optimum is the same. Inclusion of this constraint does not change the characteristic that the aircraft produce the opposite results when optimized on this 2-D space. Furthermore, this effect is pronounced enough that NDARC does not close using SUAVE's optimum location.

## VI. Conclusions/Implications

This paper illustrates some of the complexities and large uncertainties associated with modeling "clean-sheet" eVTOL aircraft with conceptual design tools. In particular, the lack of truth data based on previous designs makes calibration of empirical correlations from tools such as NDARC impossible without the use of high fidelity analysis or testing. The substantive disagreement between NDARC and SUAVE when it comes to wingspan tradeoffs suggests a closer look at the NDARC calibration as well as a comparison of the SUAVE results with Finite-Element Analysis are warranted. Interestingly, while the NDARC version of this aircraft possesses more optimistic aerodynamic assumptions, it optimizes to a more aerodynamic configuration. Conversely, while the SUAVE aircraft possesses a lower structural weight, the SUAVE models suggest that choosing a less aerodynamic and more structurally efficient design produces a lighter aircraft. These trends are in large part a result of two key differences; the first is the wing weight trade. SUAVE's wing weight estimation (from the Vahana models) takes into account spanwise loading from the rotors. As a result, decreasing wing weight becomes comparatively more important in SUAVE. NDARC's semi-empirical model does not capture the effect of this spanwise loading on the wing. The second is in large part a modeling assumption; the

relatively modest aerodynamic assumptions in SUAVE result in a battery that is large enough to meet a reasonable C-rate constraint even at high disk loadings. NDARC's aerodynamic assumptions on the other hand, are more optimistic, leading to a smaller battery that is unable to meet the C-rate constraint at high disk loadings. Nonetheless, the general agreement on the motor weight suggest that the addition of a gearbox could yield significant weight savings. However further analysis is required. The discrepancies in structural weight, aerodynamics, and motor weight merit further investigation and should be followed up on in an actual aircraft design program.

## Acknowledgments

The authors would like to thank Wayne Johnson and Chris Silva for providing the initial NDARC models as well as for their guidance and insight in writing this paper.

## References

[1] Holden, J., and Goel, N., "Uber Elevate: Fast-Forwarding to a Future of On-Demand Urban Air Transportation," Tech. rep., Uber, April 2017.

[2] Fredericks, W., Moore, M., and Busan, R., "Benefits of Hybrid-Electric Propulsion to Achieve 4x Increase in Cruise Efficiency for a VTOL Aircraft," AIAA Aviation Technology, Integration, and Operations (ATIO) Conference, Hampton, VA, 2013.

[3] Kraenzler, M., Schmitt, M., and Stumpf, E., "Conceptual Design Study on Electrical Vertical Take Off and Landing Aircraft for Urban Air Mobility Applications," *AIAA Aviation 2019 Forum*, Dallas, Tx, 2019.

[4] "Larry Page's Cora," *eFlight Journal*, Vol. 1, 2018. URL `http://www.e-flight-journal.com/e-flight-journal-aero-special-2018-small.pdf`.

[5] Clarke, M., Smart, J., Botero, E., Maier, W., and Alonso, J. J., ""Strategies for Posing a Well-Defined Problem for Urban Air Mobility Vehicles"," *AIAA 2019 Scitech Forum*, San Diego, CA, 2019.

[6] FAA, "FAA Guide to Low-Flying Aircraft," , 2017. `https://www.faa.gov/about/office_org/field_offices/fsdo/lgb/local_more/media/FAA_Guide_to_Low-Flying_Aircraft.pdf`, Accessed on 01-14-2019.

[7] Patterson, M., Antcliff, K., and Kohlman, L., "A Proposed Approach to Studying Urban Air Mobility Missions Including an Initial Exploration of Mission Requirements," *74th Annual Vertical Flight Society Forum*, Phoenix, AZ, 2018.

[8] Johnson, W., "NDARC –— NASA Design and Analysis of Rotorcraft: Validation and Demonstration," *American Helicopter Society Aeromechanics Specialists' Conference*, 2010.

[9] Johnson, W., "CAMRAD II, Comprehensive Analytical Model of Rotorcraft Aerodynamics and Dynamics," 1992.

[10] Johnson, W., "Propulsion System Models for Rotorcraft Conceptual Design," *5th Decennial AHS Aeromechanics Specialists Conference*, San Francisco, CA, 2014.

[11] Johnson, W., Silva, S., and Solis, E., "Concept Vehicles for VTOL Air Taxi Operations," *AHS Technical Conference on Aeromechanics Design for Transformative Vertical Flight*, San Francisco, CA, 2018.

[12] Johnson, W., and Silva, S. ., "Observations from Exploration of VTOL Urban Air Mobility Designs," *Seventh Asian-Australian Rotorcraft Forum*, Jeju, Korea, 2018.

[13] Lukaczyk, T., Wendorff, A. D., Botero, E., MacDonald, T., Momose, T., Variyar, A., Vegh, J. M., Colonno, M., Economon, T. D., Alonso, J. J., Orra, T. H., and Ilario da Silva, C., "SUAVE: An Open-Source Environment for Multi-Fidelity Conceptual Vehicle Design," *AIAA Aviation*, Dallas, TX, 2015.

[14] MacDonald, T., Botero, E., Vegh, J. M., Variyar, A., Alonso, J. J., Orra, T. H., and Ilario da Silva, C., ""SUAVE: An Open-Source Environment Enabling Unconventional Vehicle Designs through Higher Fidelity"," *AIAA Scitech*, Grapevine, TX, 2017.

[15] Fredericks, W., "Aircraft Conceptual Design Using Vehicle Sketch Pad," *AIAA Scitech*, Orlando, FL, 2010.

[16] Palacios, F., Colonno, M. R., Aranake, A. C., Campos, A., Copeland, S. R., Economon, T. D., Lonka, A. K., Lukaczyk, T. W., Taylor, T. W. R., and Alonso, J. J., "Stanford University Unstructured (SU2): An open-source integrated computational environment for multi-physics simulation and design," *51st AIAA Aerospace Sciences Meeting and Exhibit*, Grapevine, TX, 2013.

[17] Kroo, I., Altus, S., Braun, R., Gage, P., and Sobieski, I., "Multidisciplinary Optimization Methods for Aircraft Preliminary Design," AIAA Paper -94-4325-CP, Hampton, VA, 1994.

[18] Vegh, J. M., "Sizing Methodologies for Aircraft with Multiple Energy Systems," Ph.D. thesis, Stanford University, 2018.

[19] Botero, E., and Alonso, J. J., ""Conceptual Design and Optimization of Small Transitioning UAVs using SUAVE"," *18th AIAA/ISSMO Multidisciplinary Analysis and Optimization Conference*, Denver, CO, 2017.

[20] Leishman, J., *Principals of Helicopter Aerodynamics*, 2nd ed., Cambridge Aerospace Series, New York, New York, 2006.

[21] Bower, G., "Vahana Configuration Trade Study—-Part II," `https://vahana.aero/vahana-configuration-trade-study-part-ii-1edcdac8ad93`, 2017. Accessed on 12-06-2018.

[22] Raymer, D., *Aircraft Design: A Conceptual Approach*, 4th ed., AIAA, Playa del Ray, California, 2006.

[23] Smart, J. T., and Alonso, J. J., "Primary Weight Estimation for eVTOLs via Explicit Analysis and Surrogate Regression," *AIAA 2019 Aviation Forum*, Dallas, Texas, 2019.

[24] Gray, J. S., Moore, K. T., and Naylor, B. A., "OpenMDAO: An Open-Source Framework for Multidisciplinary Analysis and Optimization," *13th AIAA/ISSMO Multidisciplinary Analysis and Optimization Conference, Fort Worth, TX, AIAA, AIAA-2010-9101*, AIAA, Fort Worth, Texas, 2010.

[25] Meyn, L., "Rotorcraft Optimization Tools: Incorporating Rotorcraft Design Codes into Multi-Disciplinary Design, Analysis, and Optimization," *International Technical Meeting on Aeromechanics Design for Transformative Vertical Flight 2018*, American Helicopter Society (AHS), San Francisco, Ca, 2018.

[26] Stückl, S., van Toor, J., and Lobentanzer, H., "Voltair: The All Electric Propulsion Concept Platform-a Vision for Atmospheric Friendly Flight," *28th International Congress of the Aeronautical Sciences*, EADS, 2011.

[27] Vegh, J., and Alonso, J., "Design and Optimization of Short-Range Aluminum-Air Powered Aircraft," *54th AIAA Aerospace Sciences Meeting*, AIAA Scitech, San Diego, CA, 2016.

[28] Duffy, M., Wakayama, S., and Hupp, R., "A Study in Reducing the Cost of Vertical Flight with Electric Propulsion," *17th AIAA Aviation Technology, Integration, and Operations Conference*, AIAA AVIATION, Denver, Co, 2017.

[29] Gnadt, A., Speth, R., S. Sabnis, J., and R.H. Barrett, S., "Technical and environmental assessment of all-electric 180-passenger commercial aircraft," *Progress in Aerospace Sciences*, 2018.

[30] Kraft, D., "A Software Package for Sequential Quadratic Programming," *Technical Report DFVLR-FB 88-28. Oberpfaffenhofen: Institut für Dynamik der Flugsysteme*, 1998.